IOP Conf. Series: Materials Science and Engineering **114** (2016) 012132 doi:10.1088/1757-899X/114/1/012132

Tool breakage detection from 2D workpiece profile using vision method

W K Lee, M M Ratnam[1] and Z A Ahmad[2]

[1]School of Mechanical Engineering, Universiti Sains Malaysia, 14300 Nibong Tebal, Penang, Malaysia.
[2]School of Materials and Mineral Resources Engineering, Universiti Sains Malaysia, , 14300 Nibong Tebal, Penang, Malaysia.

[1]Email: mmaran@usm.my

Abstract. In-process tool breakage monitoring can significantly save cost and prevent damages to machine tool. In this paper, a machine vision approach was employed to detect the tool fracture in commercial aluminium oxide ceramic cutting tool during turning of AISI 52100 hardened steel. The contour of the workpiece profile was captured with the aid of backlighting during turning using a high-resolution DSLR camera with a shutter speed of 1/4000 s. The surface profile of the workpiece was extracted to sub-pixel accuracy using the invariant moment method. The effect of fracture in ceramic cutting tools on the surface profile signature of the machined workpiece using autocorrelation was studied. Fracture in the aluminum oxide ceramic tool was found to cause the peaks of autocorrelation function of the workpiece profile to decrease rapidly as the lag distance increased. The envelope of the peaks of the autocorrelation function was observed to deviate significantly from one another at different workpiece angles when the tool has fractured due to the continuous fracture of ceramic cutting insert during machining.

1. Introduction

Aluminium oxide based ceramic cutting tools has been widely used in hard turning, such as cast iron, martensitic stainless steel and high-temperature alloys because of their high hot-hardness and high wear resistance. However, the main drawbacks of ceramic tool material are due to their low fracture toughness and poor thermal shock resistance, thus resulting in premature tool failure by chipping or catastrophic failure by fracture instead of gradual wear [1]. Therefore, in-process detection of sudden fracture in ceramic cutting tools is very important for maintaining the stability of the machining process, avoiding the excessive damage on machine tool as well as preventing the deterioration in surface quality and dimensional accuracy of the machined parts.

Tool wear monitoring can be generally divided into two types: direct and indirect method. Direct tool condition monitoring is usually performed by means of optical such as toolmaker's microscope, scanning electron microscope, confocal microscope and white light interferometers [2-4] which can be effectively applied to quantify tool wear and tool fracture. But these methods are only feasible for offline evaluation because the cutting tool has to be dismantled from the machine tool, thereby increasing the machine downtime. Past works have been conducted for in-cycle wear measurement on cutting tools using CCD camera without the need to dismantle the cutting insert from the tool holder

[5-7]. But these methods cannot be applied in-process because the chips and coolant that interfere during machining are the major obstacle for in-process tool condition monitoring. As a result, indirect tool wear monitoring based on measurable signal features such as acoustic emission, vibration, cutting force has gained interest among researchers. It is mainly due to the indirect methods able to monitor the tool condition online which allows uninterrupted machining. These signal features are extracted through signal processing methods such as time domain, frequency domain, time-frequency domain and wavelet in order to obtain an accurate representation of the tool's state. A good review of these methods is provided by Byrne *et al* [8] and Rehorn *et al.* [9]. Cutting force is the one of the most popular sensor signals used for detecting tool breakage in turning. Cakir and Isik [10] found that the cutting force increased as tool wear increased. When cutting force increases above the preset threshold and drops suddenly, this indicated that the cutting tool has fractured because there is a total lost of contact between the cutting tool and the workpiece. However, the chipping can also cause the failure of a cutting edge without decreasing of cutting force [11]. Numerous studies have also found the monitoring of acoustic emission (AE) signal to be an effective approach to detect the tool breakage. A stepwise increase of the r.m.s of AE signal was observed after tool has fractured because of the sudden increase in the contact area between the workpiece and the fractured cutting tool [12]. However, a contradict finding was found in recent work conducted by Neslušan *et al*. [13]. They reported that conventional data processing of AE signal features do not enable the different phases of tool wear to be clearly recognised or the detection of tool breakage.

Tool condition also can be indirectly assessed based on the machined surface by using vision method. For example, Kassim *et al.* [14] and Kassim *et al*. [15] determined the degree of tool wear by analyzing the surface texture of machined captured by CCD camera using different image processing method. Their result shows that the worn tool exhibits more irregularities in the texture of machine surface compared to the new cutting tool. Liao *et al.* [16] extracted 3D workpiece surface texture parameters from the surface height map of machined workpiece and correlated with the flank wear. Dutta *et al*. [17] studied the relationship between the texture descriptors obtained from grey level co-occurrence matrix (GLCM) and the average flank wear. The surface texture of machined part showed some potential to monitor the wear of cutting tool, however, the reflection images from work piece surface is highly dependent on the reflectance of the work piece surfaces and the illumination condition of the light source. Inhomogeneous illumination due to improper lighting and interference of ambient light can cause redundant information from images. A promising method of wear assessment is by using the surface profile of the workpiece. This approach was proposed by Shahabi and Ratnam [18] for evaluating the nose wear using a CCD camera equipped with backlighting to capture the contour of the workpiece profile. The nose wear was determined by subtracting the workpiece profile generated by worn tool from the workpiece profile generated by unworn tool. However, no attempt was made to differentiate the chipping or fracture from gradual wear that commonly occur in ceramic cutting inserts.

In this paper, we propose a novel method for in-process tool fracture detection in aluminium oxide ceramic cutting insert from 2-D workpiece profile signature using machine vision method.

2. Experimental setup

2.1. Machining condition

The turning were carried on a Pinocho S90 conventional lathe machine under dry cutting condition. Commercially available aluminum oxide based ceramic insert with added zirconia (CNGA 120408T02520 CC620, Sandvik Coromant Ltd., Sweden) was used as the cutting tools. A workpiece made of AISI 52100 hardened steel was used (C: 0.98-1.1%, Mn: 0.25-0.45%, P: 0.025%, S:0025% and Cr: 1.3-1.6%). The tool holder used for the turning was DCLNR 2020M from Sandvik Coromant, Sweden. The turning operation was performed under the following cutting parameters: spindle rotational speed 950 rpm, feed rate 0.4 mm/rev and depth-of-cut 0.5 mm.

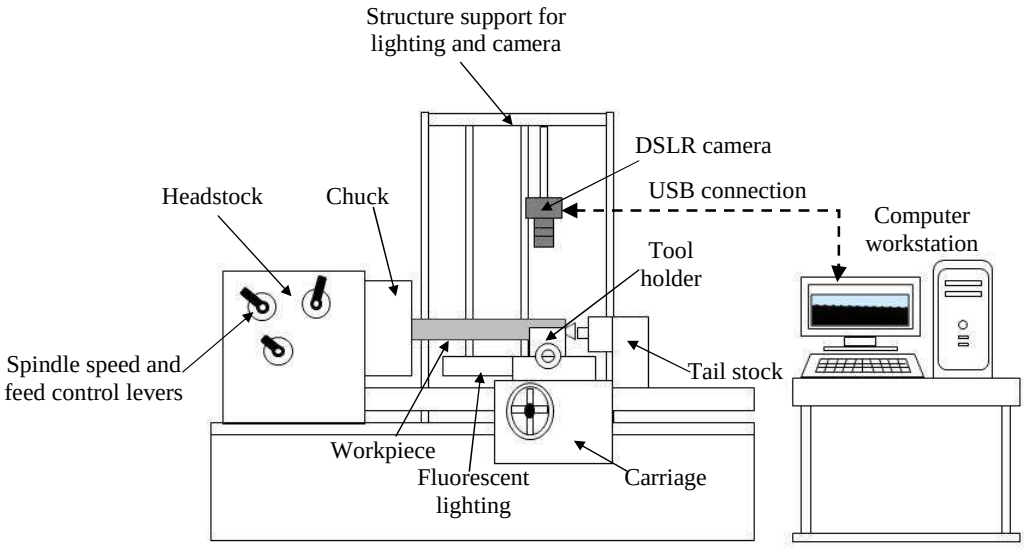

Figure 1. Schematic of image acquisition configuration

2.2. Image acquisition of workpiece profile and cutting insert

The images of the edge of workpiece were captured using a DSLR camera (model: Canon EOS 700D) fitted with Canon EF 100mm macro lens with aids of a uniform diffused backlighting illumination during the turning operation. Figure 1 shows the schematic of experiment setup. Uniform diffused backlighting illumination was obtained by using a high-frequency fluorescent light (*Edmund Optics Pte. Ltd., Singapore*) to capture a silhouette of the work piece. Shutter speed of 1/4000 s was used to freeze the motion of the rotating workpiece. The images of workpiece were captured from a remote software installed in a computer. The spindle rotation angle between each image is approximately 60^{o}. Observation on the cutting tool tip after each pass of machining was performed by using a scanning electron microscope (Hitachi TM1000 SEM) in order to observe the effect of the cutting tool condition on the autocorrelation.

2.3. Scaling factor determination and distortion assessment

The horizontal (*x*-direction) and vertical (*y*-direction) *x*- and *y*-scaling factors for converting the image coordinates in pixels to real-world coordinates in metric units were determined using standard *Mitutoyo* pin gages of known diameter (i.e. 0.25 mm, 0.725 mm and 0.895 mm). The *x*- and *y*- scaling factors were found to be f_x = 4.3179 µm/pixel and f_y = 4.2271 µm/pixel, respectively. The distortion in the image captured by the DSLR camera was evaluated by using a Ronchi ruling (50 lines/inch, *Edmund Optics Pte. Ltd., Singapore*). The image of the ruling was captured vertically and horizontally relative to the image frame where the Ronchi ruling was placed at the same level as the edge of the workpiece. The distortion in the image was determined by using the distances between selected points on the ruling. The maximum deviations in the *x*- and *y*- directions were found to be only 5 pixels (0.15%) and 3 pixels (0.06%), respectively. Therefore, the distortion effect in the image can be neglected.

2.4. Workpiece profile extraction using subpixel edge location and autocorrelation analysis

An algorithm was developed to extract the workpiece profile in sub-pixel accuracy. Firstly, the captured image was read as a RGB image and converted to grayscale image using the *Matlab* command '*rgb2gray*'. The grayscale image is composed of pixel intensity values that range from 0 (black) to 255 (white).After that, the image was further pre-processed to remove noise by using wiener

filtering. The invariant moment method proposed by Tabatabai and Mitchell [19] was applied in this study to locate the edge of workpiece profile to sub-pixel accuracy. The contour of surface roughness profile was detected using orthogonal scanning. Figure 2 shows the scanning starts from the first point of the first row to locate the sub-pixel profile on the workpiece profile. This process is repeated to detect all the sub-pixels that lie on the profile thus producing the contour of surface roughness. Because the profile of the workpiece is in pixel units, therefore the roughness profile is converted from pixel unit to micrometer by multiplying the scaling factor f_x in order to change the pixel value to micrometer.

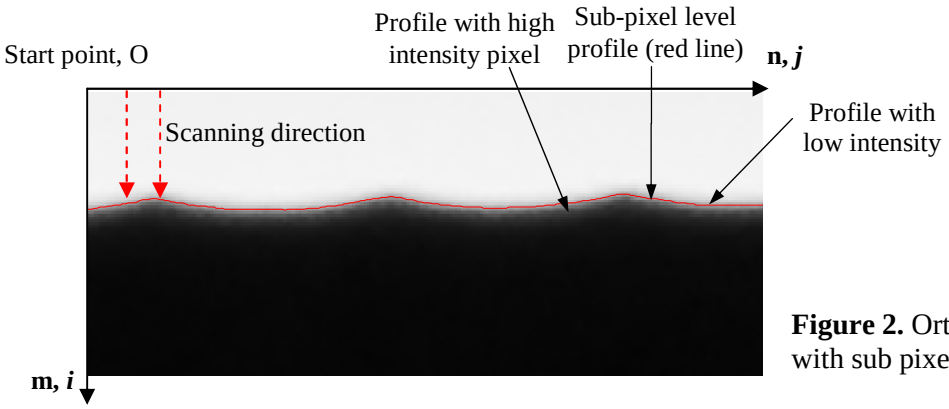

Figure 2. Orthogonal scanning with sub pixel accuracy

The extracted profile was analysed using the autocorrelation method to detect onset tool fracture by detecting the presence of the random noise buried in any periodic surface roughness profile. This was done by comparing the workpiece profile, *y(x)* with a replica of itself whereby the replica is shifted by a lag distance (τ). The autocorrelation function is the integral of the shifted and the un-shifted surface profile evaluated over the length of the profile, L and is given in Eq. (1) [20].

$$A(\tau) = \lim_{L\to\infty} \frac{1}{L} \int_0^L y(x)y(x+\tau)dx \tag{1}$$

For discrete profile data the autocorrelation function is defined as in Eq. (2)

$$A(m\Delta\tau) = \frac{1}{N} \sum_{i=1}^{N} y(i)y(i-m) \tag{2}$$

where m is an integer, N is total number of sample points on the workpiece profile, $y(i)$ is the surface profile at position $i\Delta\tau$ and $y(i-m)$ is the surface profile at position $(i-m)\Delta\tau$, i.e. at m sampling intervals earlier. The autocorrelation function is normalized by dividing $A(\tau)$ by the square of root-mean-square roughness (R_q). The root-mean-square roughness is defined as the root-mean-square average of the workpiece profile $y(i)$ calculated from the mean line and is expressed in Eq. (3).

$$R_q = \sqrt{\frac{1}{N} \sum_{i=1}^{n} y(i)^2} \tag{3}$$

3. Results and Discussion

Figures 3(a)-(d) show the peaks of the autocorrelation function against the lag distance at different rotational angles of the workpiece. From the Figure 3(a), it can be noticed that when cutting tool is

new, the envelope of the peaks of autocorrelation function decreased gradually at the beginning of machining. The envelope of the peak of autocorrelation function are almost the identical at different rotation angles. This is because the cutting tool still new and only some abrasion grooves are observed on the flank face of the cutting insert which is mainly due to the tool-workpiece abrasion in the early machining as shown in Figure 4(a). However, Figure 3(b) shows that the peak of autocorrelation decreased rapidly between lag distances of 0 mm to 8 mm at the cutting time interval between 11.1 s to 16.5 s. After that, the envelope of the peak of autocorrelation function for workpiece profile decreased irregular at different rotational angles and have significant deviation from one to another as illustrated in Figure 3(c) and Figure 3(d). This is because fracture appeared on the cutting edge of aluminum oxide ceramic inserts after machining time interval of 16.5 s as seen in Figure 4(b).

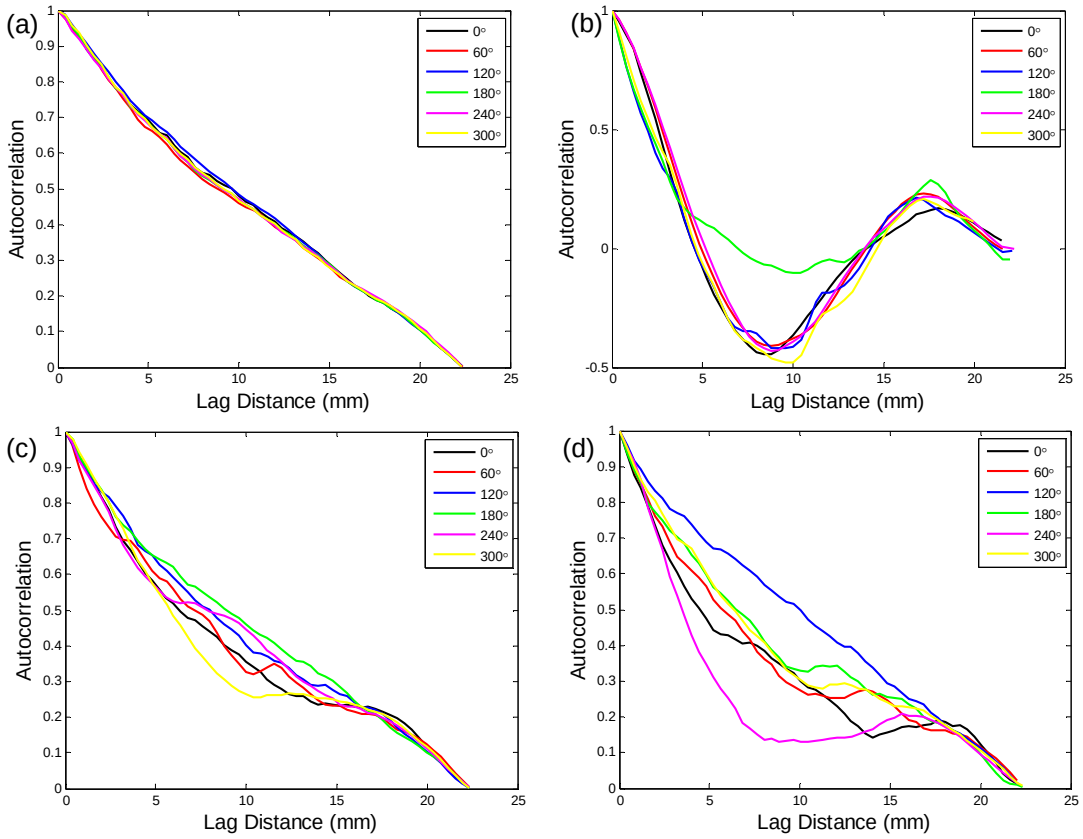

Figure 3. Peak of the autocorrelation plot at cutting time interval (a) 0-5.5s; (b) 11.1-6.5 s; (c) 16.6 - 22.0 s and (d) 22.1-27.5 s

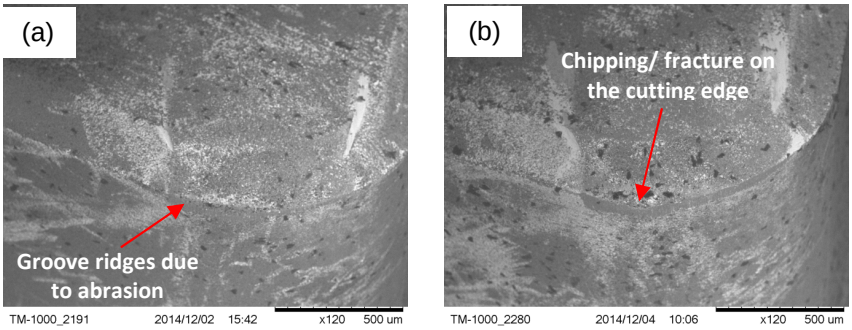

Figure 4. SEM micrograph of aluminum oxide ceramic cutting insert (a) before fracture (b) after fracture

The peaks of the autocorrelation function for a workpiece profile generated from an unworn or progressively worn cutting tool decreases gradually as a function of lag distance and are almost identical at different rotational angles as shown in Figure 3(a). This is because of the uniform and repeatable profile shows good replication of the workpiece profiles as the lag distance increased when machining with un-fractured cutting tool. It can be seen in Figure 5, the ceramic cutting insert generated a periodic profile with almost constant wavelength along the workpiece. The peak-to-valley height of the surface roughness profile was approximately constant at various rotation angles.

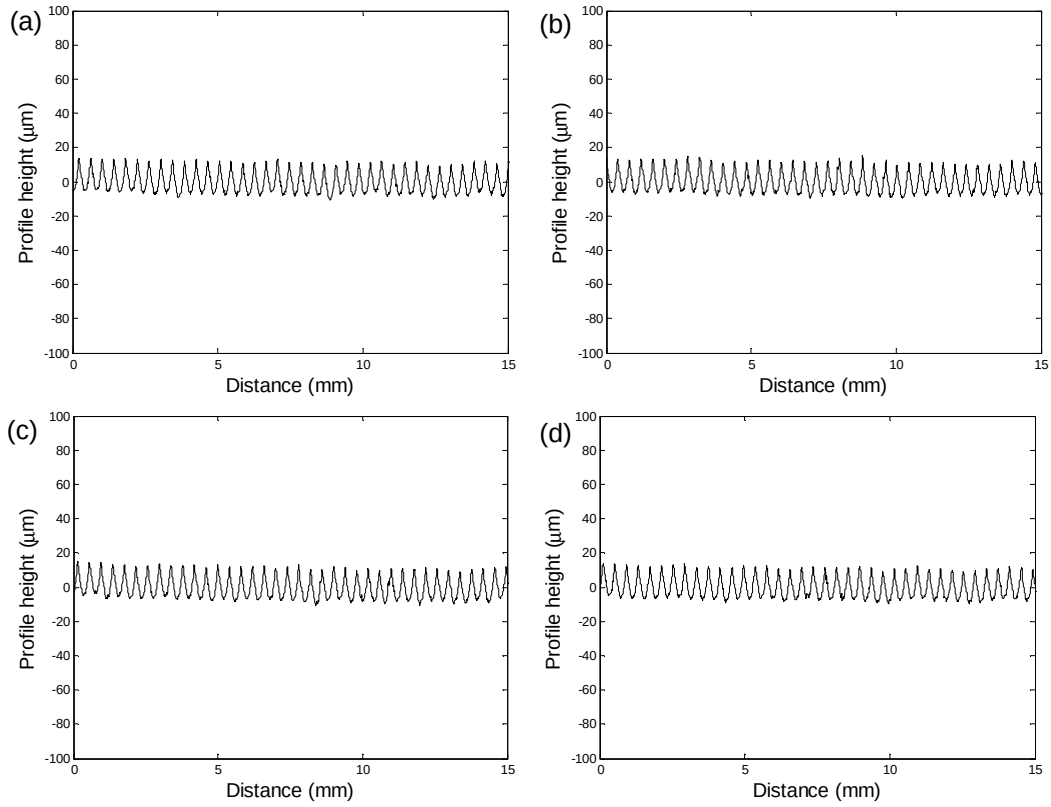

Figure 5. Extracted surface roughness profile from 2D workpiece images at different rotational angles (a) 0^o, (b)120^o, (c) 240^o, (d) 300^o in cutting time interval of 0-5.5 s

When cutting tool has fractured, a sharp decrease and a significant deviation in the peaks of the autocorrelation function for workpiece profile at different rotational angles was observed in Figure 3(c)-(d). This is mainly due to abrupt changes in the surface profile caused by fractured cutting tool and continuous failure by chipping of the cutting tool. When tool has fractured, the surface profiles do not repeat periodically compared to the profiles at the initial cutting stages which shown in Figure 6. The peak-to-valley heights of the surface roughness profile also change irregularly. When tool fracture has occurred, wider tool-workpiece contact edge area is formed and it causes the cutting force to increase. This excites the tool-workpiece to vibrate during machining [21, 22]. Consequently, vibration between fractured tool and workpiece caused unstable cutting in the tool movement with respect to the workpiece. Boryczko [23] reported that unstable of tool movement results in the non-uniform distribution of height of irregularities and displacement of wavelength in the feed direction on the workpiece profiles. This differ from the theoretical workpiece profiles to a various extent due to the complex character.

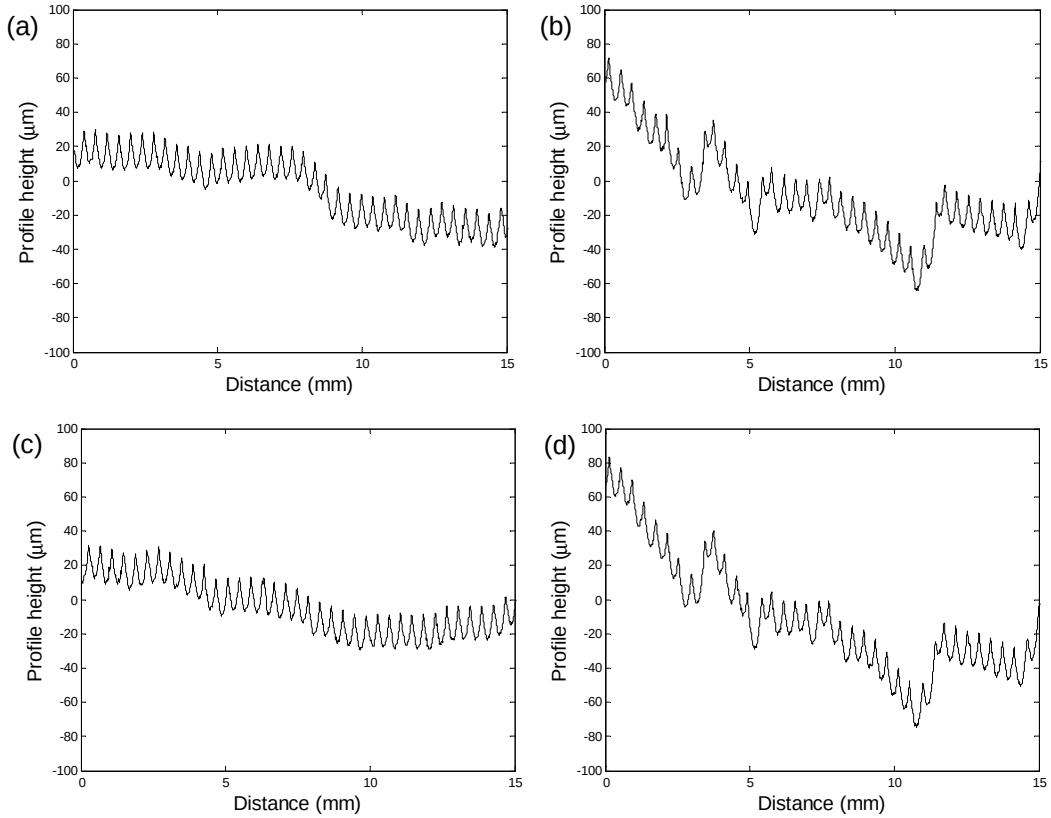

Figure 6. Extracted surface roughness profile from 2D workpiece images at different rotational angles (a) 0^o, (b)120^o, (c) 240^o, (d) 300^o in cutting time interval of 11.1-16.5

4. Conclusion

An in-process tool fracture detection system using vision method is proposed to detect the fracture of ceramic tools in turning based on the workpiece profile signature. The workpiece profile with sub-pixel accuracy was extracted and the autocorrelation function was used to investigate the effects of tool fracture on the signature of workpiece profile. The results show that the peaks of autocorrelation function of the workpiece profile generated by aluminum oxide ceramic cutting insert decreases rapidly as the lag distance increased when tool has fractured. In addition, the envelope of the peaks of the autocorrelation function was found to deviate significantly from one another at different angles after the tool has fractured.

References

[1] Grzesik W and Zalisz Z 2008 Wear phenomenon in the hard steel machining using ceramic cutting tool *Tribology Int.* **41** 802-812
[2] Devillez A, Lesko S and Mozerc W 2007 Cutting tool crater wear measurement with white light interferometry *Wear* **256** 56-65
[3] Dawson T G and Kurfess T R 2005 Quantification of tool wear using light interferometry and three dimensional computational metrology *Int. J. Mach. Tools & Manuf.* **45** 591-596
[4] Olortegui-Yume J A and Kwon P Y 2006 Tool wear evolution in multilayer coated inserts using topographic imaging *Trans.* **34** 405-412
[5] Jurkovic J, Korosec M and Kopac J 2005 New approach in tool wear measuring technique using

CCD vision system *Int. J. Mach. Tools & Manuf.* **45** 1023-30
[6] Castejón M, Algre E, Barreiro J and Hernández L K 2007 On-line monitoring using geometric descriptors from digital images *Int. J. Mach. Tools & Manuf.* **47** 1847-53
[7] Fadare D A and Oni A O 2009 Development and application of a machine vision system for measurement of tool wear *ARPN J. Eng. & Appl. Sci.* **4(4)** 42-49
[8] Byrne G, Dornfeld D, Inasaki I, Ketteler G, Konig W and Teti R. 1995 Tool condition monitoring (TCM)-the status of research and industrial application *Ann. CIRP* **44/2** 541–567
[9] Rehorn A G, Jiang J and Orban P E 2005 State-of-the-art methods and results in tool condition monitoring: a review. *Int. J. Adv. Manuf. Technol.* **26** 693-710
[10] Cakir M K and Isik Y 2005 Detecting tool breakage in turning AISI 1050 steel using coated and uncoated cutting tools *J. Mater. Process. Technol.* **159** 191-198.
[11] Jemielniak K 1992 Detection of cutting edge breakage in turning *Annal CIPR* **41** 97-100
[12] Wang H L, Shao H, Chen M and Hu D J 2003 Online tool breakage monitoring in turning. *Int. J. Adv. Manuf. Technol.* **139** 237-242
[13] Neslušan M, Mičieta B, Mičietová A, Čilliková M and Mrkvica I 2015 Detection of tool breakage during hard turning through acoustic emission at low removal rates *Measurement* **70** 1-13
[14] Kassim A A, Mian Z and Mannan M A 2004 Connectivity oriented fast Hough transform for tool wear monitoring *Pattern Recogn.* **37** 1925-33
[15] Kassim A A, Mannan M A and Mian Z 2007 Texture analysis method for tool condition monitoring *Image and Vision Comput.* **25** 1080-90.
[16] Liao Y and Stephenson D A 2010 A multifeature approach to tool wear estimation using 3D workpiece surface texture parameters *J.Manuf. Sci. Eng.* **132** 1-7
[17] Dutta S, Datta A, Das Chakladar N, Pal S K, Mukhopadhyay S and Sen R 2012 Detection of tool condition from the turned surface images using an accurate grey level co-occurrence technique *Precision Eng.* **36** 458-466
[18] Shahabi H H and Ratnam M M 2009 Assessment of flank wear and nose radius wear from workpience roughness profile in turning operation using machine vision *Int. J. Adv. Manuf. Technol.* **43** 11-21
[19] Tabatabai A J and Mitchell R 1984 Edge location to sub-pixel values in digital imagery. *IEEE Trans. Pattern Anal. Mach. Intell.* **6(2)** 188-201
[20] Bendat J S and Piersol A G 1993 Engineering application of correlation and spectral analysis *New York, Wiley*.
[21] Dimla D E 2002 The correlation of vibration signal features to cutting tool wear in a metal turning operation. *Int. J. Adv. Manuf. Technol.* **19** 705-713
[22] Dimla D E and Lister P M 2000 Online metal cutting tool condition monitoring- Part I: force and vibration analysis *Int. J. Mach. Tools & Manuf.* **40(8)** 736-768
[23] Boryczko A 2011 Profile irregularities of turned surfaces as a result of machine tool interactions *Metrol. Meas. Syst.* **18(4)** 691-700